A Novel Color Image Watermarking Algorithm Based on QWT and DCT

Shaocheng Han[1(✉)], Jinfeng Yang[2], Rui Wang[3], and Guimin Jia[2]

[1] Basic Experimental Center, Civil Aviation University of China, Tianjin 300300, China
schan@cauc.edu.cn, schan_cauc2012@163.com

[2] College of Electronic Information and Automation, Civil Aviation University of China, Tianjin 300300, China
{jfyang,gmjia}@cauc.edu.cn

[3] College of science, Civil Aviation University of China, Tianjin 300300, China
r-wang@cauc.edu.cn

Abstract. A novel color image watermarking algorithm is proposed based on quaternion wavelet transform (QWT) and discrete cosine transform (DCT) for copyright protection. The luminance channel Y of the host color image in YCbCr space is decomposed by QWT to obtain four approximation subimages. A binary watermark is embedded into the mid-frequency DCT coefficients of two randomly selected subimages. The experimental results show that the proposed watermarking scheme has good robustness against common image attacks such as adding noise, filtering, scaling, JPEG compression, cropping, image adjusting, small angle rotation and so on.

Keywords: Image watermarking · QWT · DCT · Chaotic map
YCbCr space

1 Introduction

With the rapid development of information technology, the reproduction, distribution and tampering of digital products have become common nowadays [1]. How to protect the copyright of these digital products effectively has been a hot topic in recent years. As a copyright protection technology, digital watermarking draws a lot of attentions. Because it can embed authentication information into the host image, audio and video data and also ensure the integrity and security of these data [2].

Image watermarking algorithms can be classified into spatial domain algorithms and transform domain algorithms. For the spatial domain algorithms, the watermark is usually embedded into the host image by modifying its pixels directly [3,4]. Although the spatial domain algorithms have lower computational complexity, they are fragile against some image attacks. For transform domain

J. Yang et al. (Eds.): CCCV 2017, Part I, CCIS 771, pp. 428–438, 2017.
https://doi.org/10.1007/978-981-10-7299-4_35

watermarking algorithms, the host image is firstly decomposed by some transforms, and then the watermark is embedded by modifying the coefficients after the transforms. The transform domain algorithms usually have better robustness than the spatial domain algorithms, so a lot of researchers pay more attentions to the transform domain algorithms. In recent years, the popular transform domain watermarking algorithms include Discrete Cosine Transform (DCT) [5], Discrete Fourier Transform (DFT) [6], Discrete Wavelet Transform (DWT) [7], Discrete Shearlet Transform (DST) [8] and so on.

A watermarking scheme using subsampling based on DCT was proposed by Chu et al. [9]. Many subsampling-based watermarking algorithms have been developed. In [10], a binary watermark image was permuted using Baker chaotic map. Then it was embedded into the DCT coefficients of two subimages which were selected according to a random coordinates sequence generated by a secret key. As a new multi-scale analysis tool for image representation, QWT was proposed based on Hilbert transform [11]. QWT has already been successfully applied in the field of image processing such as image denoising [12], image fusion [13], object recognition [14], and digital watermarking [15].

In this paper, a novel image watermarking scheme is proposed based on QWT and DCT. A binary watermark is scrambled by Arnold map and iterated sine chaotic system. The processes of watermark embedding and extracting are implemented on the luminance component of a host color image in YCbCr space. Instead of using subsampling, we obtain four approximation subimages of the luminance component using QWT. The signs and amplitudes of mid-frequency DCT coefficients are relatively stable to some attacks, so these coefficients are used to embed the encrypted watermark. The experimental results demonstrate the proposed scheme is more robust and effective to protect the copyright of color images.

2 Quaternion Wavelet Transform

QWT overcomes the common drawbacks of wavelet transforms by shift-invariant feature. Besides of the shift-invariant magnitude, QWT has three phases. The first two phases represent local image shifts, and the third one denotes the texture information [12]. Let $f(x,y)$ be 2-D image signal, the quaternion analytic signal is defined as follows:

$$f^q(x,y) = f(x,y) + if_{H_x}(x,y) + f_{H_y}(x,y) + kf_{H_xH_y}(x,y), \tag{1}$$

where $f_{H_x}(x,y)$ and $f_{H_y}(x,y)$ are partial Hilbert Transform respectively, $f_{H_xH_y}(x,y)$ is the total Hilbert Transform.

Suppose $\phi(x,y)$ is the scaling function, $\psi^D(x,y)$, $\psi^V(x,y)$ and $\psi^H(x,y)$ are respectively mother wavelets. If $\phi(x,y)$ and $\psi(x,y)$ are separable, the 2D QWT of $f(x,y)$ according to the quaternion analytic is defined as follows:

$$\begin{cases} \phi(x,y) = \phi_h(x)\phi_h(y) + i\phi_g(x)\phi_h(y) + j\phi_h(x)\phi_g(y) + k\phi_g(x)\phi_g(y) \\ \psi^D(x,y) = \psi_h(x)\psi_h(y) + i\psi_g(x)\psi_h(y) + j\psi_h(x)\psi_g(y) + k\psi_g(x)\psi_g(y) \\ \psi^V(x,y) = \phi_h(x)\psi_h(y) + i\phi_g(x)\psi_h(y) + j\phi_h(x)\psi_g(y) + k\phi_g(x)\psi_g(y) \\ \psi^H(x,y) = \psi_h(x)\phi_h(y) + i\psi_g(x)\phi_h(y) + j\psi_h(x)\phi_g(y) + k\psi_g(x)\phi_g(y) \end{cases}. \quad (2)$$

In other words, the coefficients of the image decomposed by QWT constitute a matrix F,

$$F = \begin{bmatrix} LL_{\phi_h(x)\phi_h(y)} & LH_{\phi_h(x)\psi_h(y)} & HL_{\psi_h(x)\phi_h(y)} & HH_{\psi_h(x)\psi_h(y)} \\ LL_{\phi_g(x)\phi_h(y)} & LH_{\phi_g(x)\psi_h(y)} & HL_{\psi_g(x)\phi_h(y)} & HH_{\psi_g(x)\psi_h(y)} \\ LL_{\phi_h(x)\phi_g(y)} & LH_{\phi_h(x)\psi_g(y)} & HL_{\psi_h(x)\phi_g(y)} & HH_{\psi_h(x)\psi_g(y)} \\ LL_{\phi_g(x)\phi_g(y)} & LH_{\phi_g(x)\psi_g(y)} & HL_{\psi_g(x)\phi_g(y)} & HH_{\psi_g(x)\psi_g(y)} \end{bmatrix}. \quad (3)$$

Each column of matrix F is corresponding to a quaternion. The first column is corresponding to the approximation subimage, and the other three columns are respectively corresponding to horizontal, vertical and diagonal subimages [14].

3 Watermarking Scheme Based on DCT and QWT

In this section, the novel watermarking embedding and extracting schemes are detailed based on DCT and QWT.

3.1 Watermark Embedding

The steps of embedding watermark into the original host color image are described as follows:

Step 1. The original watermark W is permuted by Arnold map controlled by the scrambling times K_1 to obtain the scrambled watermark W_1.

Step 2. A random sequence $X_1 = \{x_n \,|\, n = 1, 2, \ldots, L\}$ is generated by the iterated sine chaotic map which is defined as

$$x_{n+1} = \sin\left(\varepsilon \arcsin\sqrt{|x_n - 1|}\right), \quad (4)$$

and then X_1 is converted into a binary sequence G_1 by comparing with the threshold T.

Step 3. W_1 is converted into a vector $\widetilde{W}$ by zigzag scanning. Then we do XOR operation on $\widetilde{W}$ with G_1 to obtain the vector $\overline{W}$. $\overline{W}$ is divided into $\overline{W}_1$ and $\overline{W}_2$ as the final watermark information. The above process is shown as

$$\begin{cases} \overline{W} = \widetilde{W} \oplus G_1 \\ \begin{cases} \overline{W}_1 = \overline{W}(1:L/2) \\ \overline{W}_2 = \overline{W}(L/2+1:L) \end{cases} \end{cases}. \quad (5)$$

Step 4. The original host image I is converted from RGB space into YCbCr space. The luminance component Y is decomposed by 2-level QWT transform to obtain one magnitude low-frequency subimage and three phase low-frequency subimages, denoted by D_1, D_2, D_3 and D_4.

Step 5. D_1, D_2, D_3 and D_4 are decomposed by 2D-DCT transform, and the transformed coefficients are zigzag scanned into four vectors respectively, denoted by V_1, V_2, V_3 and V_4.

Step 6. Two random sequences X_2 and X_3 are generated following the step2, where the length of X_2 and X_3 are both $L/2$. For every x_n of X_2 or X_3, we set $g_n = \text{ceil}(4 * x_n)$ to obtain G_2 and G_3. According to G_2 and G_3, we construct a sequence of random number pairs $Z_1 = \{(i,j) \,|\, i \neq j \text{ and } i,j \in \{1,2,3,4\}\}$, where the length of Z_1 is $L/2$.

Step 7. According to Z_1, a complementary sequence with random number pairs $Z_2 = \{(x,y)\}$ is determined. For instance, if $(i,j) = (1,4)$ in Z_1, then (x,y) must be $(2,3)$ or $(3,2)$ in Z_2. Z_1 and Z_2 are used to select which two vectors of V_1, V_2, V_3 and V_4 to embed the watermark $\overline{W}_1$ and $\overline{W}_2$ respectively.

Step 8. Because the process of embedding $\overline{W}_1$ into V_i and V_j is same to that of embedding $\overline{W}_2$ into V_x and V_y, we take embedding $\overline{W}_1$ into V_i and V_j as an example to describe the process of watermark embedding:

Firstly, we select two vectors V_i and V_j based on Z_1 so that $V_i(k) \geqslant V_j(k)$ if $\overline{W}_1(k) = 1$ and $V_i(k) < V_j(k)$ if $\overline{W}_1(k) = 0$:

$$Z_1'(k) = \begin{cases} Z_1(k)\{i \leftrightarrow j\} & \text{if } \overline{W}_1(k) = 1 \ \& \ V_i(k) < V_j(k) \\ Z_1(k)\{i \leftrightarrow j\} & \text{if } \overline{W}_1(k) = 0 \ \& \ V_i(k) \geq V_j(k) \end{cases}, \tag{6}$$

where $Z_1(k)\{i \leftrightarrow j\}$ means swapping i and j for the k-th number pairs in Z_1.

Secondly, we re-select the k-th pair coefficients based on Z_1', and calculate the following equations

$$d_1 = |V_i(a_1 + k)| + |V_j(a_1 + k)|\,,\ d_2 = |V_i(a_1 + k) - V_j(a_1 + k)|\,. \tag{7}$$

Finally, the watermark embedding algorithm is given as

$$\begin{cases} \begin{cases} V_i'(a_1 + k) = V_i(a_1 + k) + \alpha\left(2\overline{W}_1(k) - 1\right) d_1 \\ V_j'(a_1 + k) = V_j(a_1 + k) - \alpha\left(2\overline{W}_1(k) - 1\right) d_1 \end{cases} & \text{if } d_2/d_1 \leq \beta \\ V_i'(k) = V_i(k),\ V_j'(k) = V_j(k) & \text{else} \end{cases}, \tag{8}$$

where a_1 means the first position of the selected coefficients, α and β are two strength parameters.

Step 9. Inverse zigzag scanning and inverse DCT are applied to V_1', V_2', V_3' and V_4' to obtain four watermarked low-frequency sub-images. After the inverse QWT, the watermarked luminance component Y' is obtained. Then we compose Y' with the other two components to obtain the watermarked image I_1.

3.2 Watermark Extraction

The detailed steps of watermark extracting are described as follows:

Step 1. Suppose the watermarked image which undergone some attacks is I_2. I_2 is converted from RGB space to YCbCr space. Then we obtain the luminance component of watermarked image, denoted by Y_1.

Step 2. Y_1' is decomposed by 2-levels QWT transform to obtain one magnitude low-frequency subimage and three phase low-frequency subimages, denoted by D_1^*, D_2^*, D_3^* and D_4^*.

Step 3. D_1^*, D_2^*, D_3^* and D_4^* are decomposed by 2D-DCT transform, and the transformed coefficients are zigzag scanned into four vectors respectively, denoted by U_1, U_2, U_3 and U_4.

Step 4. Two vectors U_i and U_j are selected according to Z_1 or Z_2. The extracted watermark $\hat{W}_1$ or $\hat{W}_2$ can be obtained as follows:

$$\hat{W}_l(k) = \begin{cases} 1 & \text{if } U_i(a_1+k) \geqslant U_j(a_1+k) \\ 0 & \text{else} \end{cases}, \tag{9}$$

where $l = 1, 2$.

Step 5. $\hat{W}_1$ is combined with $\hat{W}_2$. Then the final extracted watermarked W' is obtained

$$W' = \text{Arnold}^{-1}\left(\text{zigzag}^{-1}\left(\hat{W} \oplus G_1\right)\right). \tag{10}$$

4 Experimental Results

The experimental results of the proposed watermarking scheme are presented in this section. Three 512×512 RGB color images in Fig. 1(a)–(c) are used as test images. A 64×64 binary logo image in Fig. 1(d) is used as the original watermark. In the experiments, we set the initial values x_0 and factors ε to 0.6345, 0.5872, 0.4536 and 2.356, 2.123, 2.678 for X_1, X_2, X_3 respectively. The threshold T is set to 0.5. The parameter a_1 in Eqs. (7) and (8) is set to 200. The parameters α and β in Eq. (8) are set to 0.4 and 0.2.

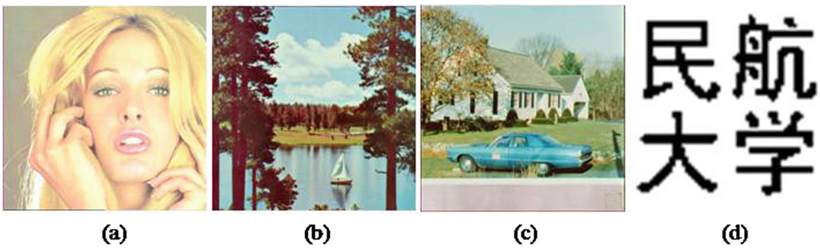

Fig. 1. (a) Host Tiffany image; (b) Host Sailboat image; (c) Host House image; (d) Original watermark.

4.1 Imperceptibility Test

The imperceptibility means that the human visual quality of original host image should not be affected much even after watermark embedding [5]. The peak value signal to noise ratio (PSNR) is used as objective criteria to evaluate the quality of the watermarked image. The PSNR for color image can be calculated as follows:

$$\text{PSNR} = \frac{1}{3}\sum_{c} 10\,\log_{10} \frac{N^2 P^2}{\sum_{x=1}^{N}\sum_{y=1}^{N}\left(I(x,y) - I'(x,y)\right)^2}, \tag{11}$$

where I and I' are the host image and watermarked image respectively, N denotes the size of I and I', P is their peak value, and $c \in \{R, G, B\}$ denotes each component of color image.

The proposed scheme shows high imperceptibility, as shown in Fig. 2, where high PSNR values are achieved for the host test images, such as Tiffany image (55.4122 dB), Sailboat image (48.4961 dB), House image (49.7479 dB).

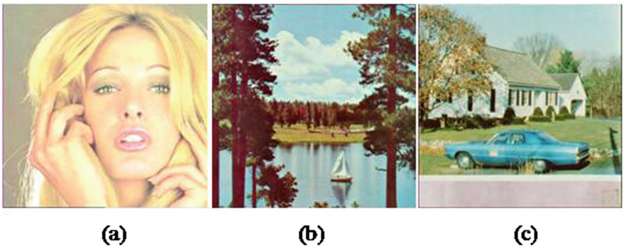

Fig. 2. (a) Watermarked Tiffany image; (b) Watermarked Sailboat image; (c) Watermarked House image.

4.2 Robustness Test

Robustness is an important requirement for any watermarking system. In this paper, the normalized cross-correlation (NC) is employed to evaluate the robustness of the algorithms. The NC is defined as

$$\text{NC}(W, W') = \frac{\sum_{i=1}^{M}\sum_{j=1}^{M} W(i,j)W'(i,j)}{\sqrt{\sum_{i=1}^{M}\sum_{j=1}^{M} W^2(i,j)}\sqrt{\sum_{i=1}^{M}\sum_{j=1}^{M} W'^2(i,j)}}, \tag{12}$$

where M represents the size of the watermark, W and W' indicate the original watermark and the extracted watermark. The NC value ranges from 0 to 1. If the NC value is near to 1, it means that the extracted watermark is strong correlate to the original watermark. But if it is near to 0, it means that the extracted watermark is almost uncorrelated. If the similarity between the original watermark and the extracted watermark is higher, the NC value is larger, which indicates that the algorithm is more robust. Generally, the NC value is considered acceptable if it is not less than 0.75.

The proposed scheme has strong robustness. This can be proved by extracting the watermark image and calculating NC between the original watermark and the extracted watermark after image attacks. In Fig. 3, we show some watermarked Tiffany images which have undergone the attacks of (a) Gaussian noise (0.03), (b) Speckle noise (0.1), (c) Pepper & Salt noise (0.1), (d) Median filter (7×7), (e) Scaling (512–64–512), (f) JPEG compression $Q = 5$, (g) Cropping (1/32 upper left corner), (h) Rows deleting (101–130), (i) Right translation by two columns, (j) Image adjusting ([0.3 0.7] $\rightarrow$ [0 1]), (k) Brightening (-80), and (l) Turn right rotation (1°). Compared with the original Tiffany image, the watermarked Tiffany images in Fig. 3 have changed a lot after these attacks. The corresponding extracted watermarks from the attacked images in Fig. 3 are shown in Fig. 4. It is shown that the proposed scheme has strong robustness, since the extracted watermarks in Fig. 4 are basically clear.

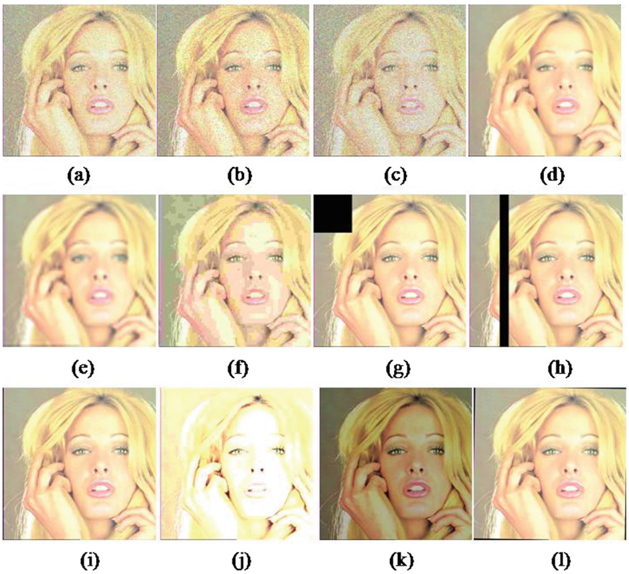

Fig. 3. Watermarked Tiffany images under different attacks

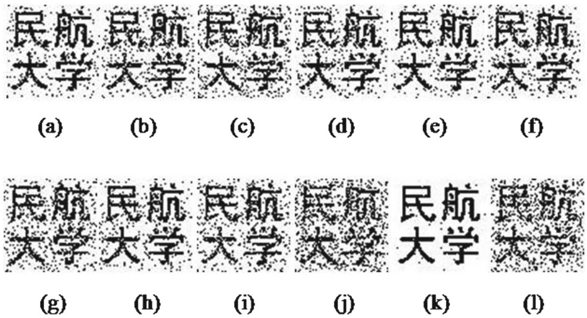

Fig. 4. Extracted watermarks from watermarked Tiffany images under different attacks

4.3 Comparative Analysis and Discussion

The binary watermark is embedded into the luminance component in YCbCr space and YUV space respectively in [16,17]. The host images are 512×512 gray-scale images in [10]. In our experiments, the binary watermark is embedded into the luminance components of host color images in YCbCr space by Lu's method in [10]. In Table 1, Figs. 5 and 6, the proposed method shows the strongest robustness, especially in adding noise, filtering, scaling, JPEG compression and rotation attacks for different color images.

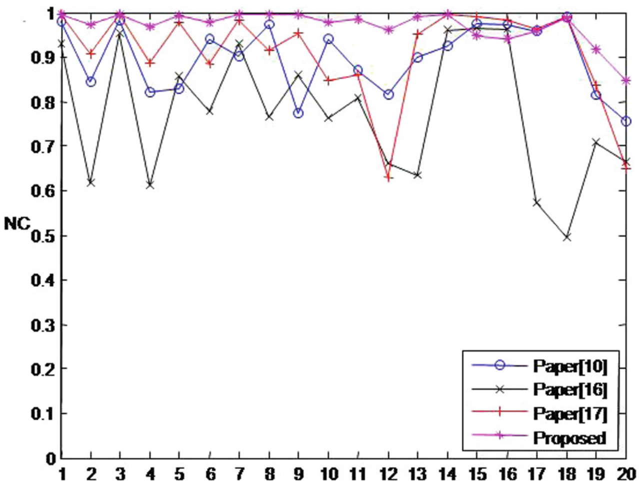

Fig. 5. Robustness comparison in different schemes for Sailboat image

Table 1. NC values comparison in different schemes for Tiffany image

No.	Attacks	Paper [10]	Paper [16]	Paper [17]	Proposed
1	Gaussian noise (0.001)	0.9418	0.7244	0.8828	0.9908
2	Gaussian noise (0.03)	0.7745	0.6231	0.8071	0.9487
3	Pepper & Salt noise (0.02)	0.9442	0.7473	0.8902	0.9908
4	Pepper & Salt noise (0.1)	0.7381	0.6171	0.7972	0.9345
5	Median filter (3 × 3)	0.8273	0.7452	0.8652	0.9859
6	Median filter (5 × 5)	0.9063	0.7108	0.8101	0.9558
7	Wiener filter (3 × 3)	0.8852	0.7675	0.8723	0.9959
8	Wiener filter (5 × 5)	0.9551	0.7275	0.8344	0.9927
9	Average filter (3 × 3)	0.7406	0.7481	0.8441	0.9895
10	Average filter (5 × 5)	0.8967	0.7118	0.7894	0.9721
11	Scaling (512–128–512)	0.8261	0.7371	0.8029	0.9743
12	Scaling (512–64–512)	0.7713	0.6448	0.5978	0.9548
13	JPEG compression $Q = 20$	0.8738	0.5658	0.8386	0.9840
14	JPEG compression $Q = 50$	0.9001	0.7412	0.8798	0.9911
15	Cropping (1/16 upper left corner)	0.9792	0.7308	0.8829	0.9105
16	Columns deleting (101–130)	0.9587	0.7439	0.8814	0.9474
17	Image adjusting ([0.3 0.7]→[0 1])	0.8961	0.5537	0.9399	0.8637
18	Brightening (+50)	0.9416	0.5956	0.9278	0.9233
19	Rotation (Right 0.5°)	0.8132	0.6574	0.7589	0.9265
20	Rotation (Right 1°)	0.7533	0.6218	0.6011	0.8746

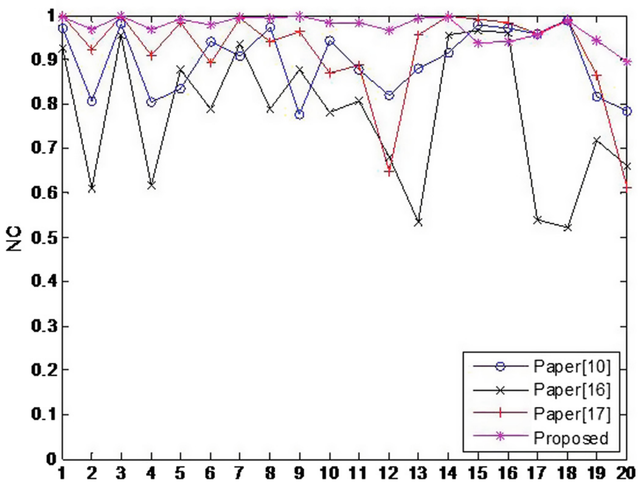

Fig. 6. Robustness comparison in different schemes for House image

5 Conclusion

In this paper, a novel color image watermarking algorithm has been proposed based on QWT and DCT. The Arnold map and iterated sine chaotic system are used to encrypt the watermark to increase the security of this algorithm. The luminance component of host color image in YCbCr space is decomposed by QWT firstly. Then the encrypted watermark has been embedded into the mid-frequency DCT coefficients of two random approximation subimages. The experimental results have shown that the proposed method attains more excellent imperceptibility and has stronger robustness against some attacks than the watermarking schemes in [10,16,17]. In future, we will extend the proposed watermarking scheme to the video watermarking.

Acknowledgments. This work was partially supported by the National Natural Science Foundation of China (Grant Nos. 61379102, U1433105, U1433120 and 61502498).

References

1. Hu, H.T., Hsu, L.Y.: A mixed modulation scheme for blind image watermarking. AEU - Int. J. Electron. Commun. **70**(2), 172–178 (2015)
2. Leung, H.Y., Cheng, L.M.: Robust watermarking scheme using wave atoms. EURASIP J. Adv. Sig. Process. **2011**(1), 1–9 (2011)
3. Karybali, I.G., Berberidis, K.: Efficient spatial image watermarking via new perceptual masking and blind detection schemes. IEEE Trans. Inf. Forensics Secur. **1**(2), 256–274 (2006)
4. Nasir, I., Weng, Y., Jiang, J., Ipson, S.: Multiple spatial watermarking technique in color images. SIViP **4**(2), 145–154 (2010)
5. Das, C., Panigrahi, S., Sharma, V.K., Mahapatra, K.K.: A novel blind robust image watermarking in DCT domain using inter-block coefficient correlation. AEU - Int. J. Electron. Commun. **68**(3), 244–253 (2014)
6. Urvoy, M., Goudia, D., Autrusseau, F.: Perceptual DFT, watermarking with improved detection and robustness to geometrical distortions. IEEE Trans. Inf. Forensics Secur. **9**(7), 1108–1119 (2014)
7. Keyvanpour, M.R., Bayat, F.M.: Blind image watermarking method based on chaotic key and dynamic coefficient quantization in the DWT domain. Math. Comput. Model. **58**(1–2), 56–67 (2013)
8. Mardanpour, M., Chahooki, M.A.Z.: Robust transparent image watermarking with Shearlet transform and bidiagonal singular value decomposition. AEU - Int. J. Electron. Commun. **70**(6), 790–798 (2016)
9. Chu, W.C.: DCT-based image watermarking using subsampling. IEEE Trans. Multimedia **5**(1), 34–38 (2003)
10. Lu, W., Lu, H., Chung, F.: Robust digital image watermarking based on subsampling. Appl. Math. Comput. **181**(2), 886–893 (2006)
11. Bayro-Corrochano, E.: Multi-resolution image analysis using the quaternion wavelet transform. Numer. Algorithms **39**(1), 35–55 (2005)
12. Yin, M., Liu, W., Shui, J., Wu, J.: Quaternion wavelet analysis and application in image denoising. Math. Probl. Eng. **2012**(1), 587–612 (2012)

13. Pang, H., Zhu, M., Guo, L.: Multifocus color image fusion using quaternion wavelet transform. In: International Congress on Image and Signal Processing, pp. 543–546. IEEE (2012)
14. Priyadharshini, R.A., Arivazhagan, S.: A quaternionic wavelet transform-based approach for object recognition. Def. Sci. J. **64**(4), 350–357 (2014)
15. Lei, B., Ni, D., Chen, S., Wang, T., Zhou, F.: Optimal image watermarking scheme based on chaotic map and quaternion wavelet transform. Nonlinear Dyn. **78**(4), 2897–2907 (2014)
16. Su, Q., Niu, Y., Wang, Q., Sheng, G.: A blind color image watermarking based on DC component in the spatial domain. Optik - Int. J. Light Electron Opt. **124**(23), 6255–6260 (2013)
17. Liu, N., Li, H., Dai, H., Chen, D.: Robust blind image watermarking based on chaotic mixtures. Nonlinear Dyn. **80**(3), 1329–1355 (2015)